Model for minority carrier lifetimes in doped HgCdTe

S. Krishnamurthy, M. A. Berding, Zhi Gang Yu
SRI International, Menlo Park, CA

C. H. Swartz and T. H. Myers

Physics Department, West Virginia University, Morgantown, WV

D. D. Edwall and R. DeWames

Rockwell Scientific Company, Thousand Oaks, CA

Abstract

We calculate the radiative, Auger and the Shockley-Read-Hall recombination rates with Fermi-Dirac statistics and accurate band structures to explain the measured temperature-dependence and doping-dependence of minority carrier lifetimes in three n and one p-type samples. We show that a trap state tracking the conduction band edge with very small activation energy can explain the lifetimes in the n-doped samples considered here. Similarly, for moderately p-doped HgCdTe alloy, a trap level at 75 meV is needed to explain the observed lifetimes. In either case, movement of Fermi level with respect to the trap level explains the temperature-dependence of the lifetimes.

Key words: Minority carrier lifetimes, Shockley-Read-Hall, Fermi-Dirac statistics, HgCdTe, trap states.

Introduction

High-performance HgCdTe infrared detectors depend on long minority carrier lifetimes in the material. In a recent study, we measured temperature-dependent photoconductance lifetimes in n-doped and nominally undoped HgCdTe grown by molecular beam epitaxy (MBE).[1] To understand the impact of various post-growth anneals on the properties of HgCdTe, we subjected the samples discussed in that paper to either a standard single-step anneal (10 hours at 245ºC) or a two-step anneal (several minutes at 430°C, followed by an *n*-type conversion anneal). We correlated these lifetime measurements with results of variable magnetic-field Hall measurements on the same samples to develop a better understanding of the performance-limiting materials properties of infrared devices.

In this paper we interpret the HgCdTe lifetime data reported in Ref [1]. Three primary mechanisms limit the lifetimes in bulk semiconductor materials: radiative recombination, Auger recombination, and SRH recombination. In this paper we use a semi empirical Hamiltonian to obtain accurate band structures and electronic wave functions for the HgCdTe narrow gap alloys. The radiative and Auger recombination rates are calculated directly from the alloy wave functions. In earlier work we developed a methodology to predict the SRH recombination rate arising from intrinsic (native) defects.[2] However, in most materials, extrinsic (impurity) defects that will also serve as recombination centers are also present. Because of uncertainty about the identity and properties (density, cross section, and location in the band gap) of impurity states that might be present, in this paper the SRH center properties are treated as parameters in the SRH recombination rate equations that have been generalized for degenerate semiconductors.

Theoretical Approach

HgCdTe Band Structures

Our calculations of the Auger and radiative recombination lifetimes use the full band structures of HgCdTe. Zero-temperature band structures of HgTe and CdTe are calculated using a long-range hybrid pseudopotential tight-binding (HPTB) Hamiltonian.[3] A small perturbation Hamiltonian is added and adjusted to provide band structure properties, including the spin-orbit splitting at the top of the valence band, in good agreement with measured values. We find that the correction to bands from the alloy disorder is small near the band edge, and hence only the virtual crystal approximation (VCA) is used to obtain the alloy band structures.[3] The localized tight-binding basis orbitals are expanded in a series of plane waves, and relevant scattering matrix elements are calculated between the plane waves in the basis set.

Because we are interested in studying lifetimes over a wide range of temperatures from ~20 K up to room temperature, it is important to include the temperature dependence of the alloy band structures in our calculations. Direct calculation of the temperature-dependent alloy band structures is computationally time consuming. Instead, we capture the temperature dependence for a given temperature T and composition x of interest by using the zero-temperature wave functions ψ and band energies E_m^k of the composition x' that has the same band gap. Thus

$$\psi(T,x) \leftarrow \psi(0,x')$$

$$E_m^k(T,x) \leftarrow E_m^k(0,x')$$

This is expected to be a good assumption over the range of temperatures and compositions of interest here. The expression by Hansen, Schmit, and Casselman[4] for $E_g(x,T)$ is used in this

mapping. Intrinsic carrier densities predicted by our band structures are in good agreement with those given by Hansen and Schmit[5] and those measured at WVU. The x values for the alloys are deduced from the band gap measurements on the samples taken at Rockwell.

Lifetime Calculations

Radiative Recombination

Radiative recombination (RR) is the process through which an electron and hole recombine, with the excess energy being accommodated by the emission of a photon. Although direct calculation of the radiative recombination rates from the quantum mechanical treatment is straightforward in principle, in practice the rates are usually deduced from the optical absorption coefficient, using the principle of detailed balance, as originally discussed by van Roosbroeck and Shockley.[6] The expressions are typically obtained with several approximations. For example, the expression reported in the review by Lopes et al.[7] for radiative recombination rates, taken from Schacham and Finkman,[8] are derived from an expression for the absorption coefficient that assumes parabolic, effective mass-like conduction and valence bands.[9] In the narrow gap HgCdTe band structures, both conduction and valence bands are far from effective mass-like. While the valence band is highly anisotropic, the conduction band character is more hyperbolic than parabolic. We calculated the radiative recombination rates directly from the electronic band structures that have the anisotropy and nonparabolicity built into them. The near band-edge absorption coefficient in HgCdTe was calculated using this band structure and is reported elsewhere.[10] The recombination lifetime τ_{rad} in n-doped material is defined as a ratio of the radiative recombination rate R_{rad} to the hole density p,

$$\frac{1}{\tau_{rad}} = \frac{0.8672\times10^{10}\,\frac{n^3}{\varepsilon_\infty a^2}\left(\sum_{m=1}^{8}\sum_{k}\left(1-f\left(E_m^k,F_0\right)\right)\sum_{n=9}^{16}\left(f\left(E_n^k,F_0\right)\left|\left\langle m\vec{k}\right|p\left|n\vec{k}\right\rangle\right|^2\left(\frac{E_n^k-E_m^k}{1-e^{-(E_m^k-E_n^k)/kT}}\right)\right)\right)}{\sum_{m=1}^{8}\left(\sum_{\vec{k}}\left(1-f\left(E_m^k,F_0\right)\right)\right)}$$

All energies are in eV, crystal wave vector k is (2π /a), lattice constant a is in Angstrom, and crystal momentum p is in (h/a). The *m* and *n* sums are over the eight valence and conduction bands, respectively; the *k* sum is over the entire Brillouin zone and captures the density of states in these bands. The $f\left(E_m^k, F_0\right)$ is the Fermi Dirac distribution function that determines the occupation of the state at $\vec{k}$ in the mth energy bands, and with the Fermi energy F_0. The term $\left\langle m\vec{k}\right|$ is the wave function for the mth band with wave vector $\vec{k}$ and energy E_m^k, and similarly for $\left|n\vec{k}\right\rangle$. The prefactor includes the number density *n* in units of cm^{-3}, the high frequency dielectric constant ε_∞, and the lattice constant *a* in Angstroms. The expression for *p*-doped material is the same, except that the denominator in the above expression will be replaced by minority carrier electron density.

Auger Recombination

Auger recombination (AR) in *n*-type material, the so called "Auger 1" process, involves three carriers: An electron in the conduction band recombines with a hole in the valence band, and the excess energy excites a second electron into a higher energy state in the conduction band. As is the case for radiative recombination, the analytical quantum mechanical expressions for the Auger recombination rates are straightforward to write down. However, evaluation of the rates is usually difficult, because it not only requires evaluation of matrix elements involving the

electronic wave functions, but also involves a triple integral over the Brillouin zone—a numerically tedious and computationally time-consuming task.

In practice, the Auger rates are usually calculated from expressions such as that reported in Lopes et al.[7] and taken from Blakemore.[11] In these expressions, effective mass-like densities of states are assumed for both valence and conduction band, and the lifetimes are

$$\frac{1}{\tau_{Auger}} \propto \left|F_1 F_2\right|^2$$

where F_1 and F_2 are overlap integrals of the Bloch functions. Although the overlap integrals are known to depend on the wave vector k,[12] they are usually taken as parameters ranging from ~0.1 to ~0.3, adjusted to fit measured lifetimes.

In our previous work[13,14] we reported on the Auger lifetimes using our HPTB band structures in a number of semiconductors, including both *p*-type (Auger 7) and *n*-type (Auger 1) HgCdTe. In that work the Auger recombination rate was calculated from second-order perturbation theory. The Auger lifetime τ_{Auger} is given by

$$\frac{1}{\tau_{Auger}} = \frac{1}{p}\int d^3k_1 \int d^3k_2 \int d^3k_3 \xi \delta\left(E_{k_1} + E_{k_2} - E_{k_3} - E_{k_1+k_2-k_3}\right)$$

$$\times f(E_{k_1}, F_0) f(E_{k_2}, F_0)\left(1 - f(E_{k_3}, F_0)\right)\left(1 - f(E_{k_1+k_2-k_3}, F_0)\right)$$

where k_1 and k_2 are the initial electron states in the conduction band, and k_3 is the initial hole state. The detailed expression for ξ is given in Ref. [13]; we note here that it includes contributions from both Coulomb-and phonon-mediated interactions of the charge carriers. The calculational procedure discussed in Ref. [13] is applied to the alloy compositions, doping

concentrations, and temperatures of interest here. A nearly identical expression is obtained for Auger 7 recombination times in *p*-doped material, as described in Ref. [14].

Shockley-Read-Hall Recombination

A commonly used expression for the SRH recombination lifetime in nondegenerate *n*-type material under low injection conditions is[15]

$$\tau_{SRH} = \frac{1}{\sigma_p N_t v_{th}^p}$$

where N_t is the number of traps, σ_p is trap cross sections for hole capture, and v_{th}^p is the averaged thermal velocities of holes in the valence band. The above textbook expression is not sufficient to accurately describe SRH in narrow gap HgCdTe, both because of the need to use degenerate statistics and because of the large variation in the band gap with temperature and resulting unusual temperature dependence of the Fermi level.

Following the procedure described in the original papers on SRH recombination,[16] we obtained a generalized expression for SRH lifetimes in degenerate semiconductors. The functional form is identical to the original expression, but differs in important details. The general expression for the net SRH recombination rate is given by

$$R_{SRH} = \frac{c_n c_p (np - n_1 p_1)}{c_n (n + n_1) + c_p (p + p_1)}$$

where $n = \int_{E_C}^{\infty} f(E, F_n) \rho_C (E) dE$ and $p = \int_{-\infty}^{E_V} (1 - f(E, F_p)) \rho_V (E) dE$ are the concentration of electrons and holes in the conduction and valence bands, respectively. In this expression, ρ_c and ρ_v are the conduction and valence band densities of states, E_c and E_v are the energies of the

conduction and valence band edges, and F_n and F_p are the quasi-Fermi levels for electrons and holes. The terms n_1 and p_1 are defined as $n_1 = ne^{\beta(E_t - F_n)}$ and $p_1 = pe^{-\beta(E_t - F_p)}$, and $c_n = N_t \sigma_n v_{th}^n$ and $c_p = N_t \sigma_p v_{th}^p$ are related to the probabilities of capture of an electron in the conduction band and a hole in the valence band by N_t traps.

The carrier density n (p) can be written as the sum of equilibrium charge density n_0 (p_0) for the Fermi level at the equilibrium position, F_0, and the photoexcited density, $\Delta n = \Delta p$. In n-type material $n \approx n_0$ because $n_0 >> \Delta n$ at low excitation intensities. Furthermore, because the density of photoexcited electrons and holes is low, and $m^*_e << m^*_h$, the Fermi level is always near to the conduction band edge and Boltzmann statistics can be applied to the hole concentrations. Dropping terms of order Δp^2, we obtain for the SRH limited lifetime for holes in *n*-type material, $\tau_{SRH} = \Delta p / R_{SRH}$ and

$$\tau_{SRH} = \frac{(1+\eta) + \left(\frac{\sigma_p v_{th}^p}{\sigma_{np} v_{th}^n}\right)\left(\frac{p_0}{n_0}\right)\left(\frac{p}{p_0} + \frac{1}{\eta}\right)}{\sigma_p N_t v_{th}^p \left(1 + \frac{p_0}{n_0}\right)} \approx \frac{(1+\eta) + \left(\frac{v_{th}^p}{v_{th}^n}\right)\left(\frac{p_0}{n_0}\right)\left(1 + \frac{1}{\eta}\right)}{\sigma_p N_t v_{th}^p \left(1 + \frac{p_0}{n_0}\right)}$$

where $\eta = e^{\beta(E_t - F_0)}$. In the second term in the numerator, the replacement of p/p_0 by 1 is justified at high temperatures because $p \approx p_0$. At low temperatures p_0 / n_0 is very small, so the contribution from the second term in the numerator is negligible and the first term dominates. For simplicity we have assumed $\sigma_n \approx \sigma_p$. The HPTB band structures are used to obtain F_0, n_0, and p_0 as functions of temperature and of alloy and doping concentration. The average thermal velocity of electrons and holes is calculated from the corresponding density of states, averaged

using the appropriate Fermi-Dirac distribution function. The expression for minority electrons in p-doped material takes the following form, where $\varsigma = e^{-\beta(E_t - F_0)}$

$$\tau_{SRH} = \frac{(1+\varsigma) + \left(\frac{\sigma_n v_{th}^n}{\sigma_p v_{th}^p}\right)\left(\frac{n_0}{p_0}\right)\left(\frac{n}{n_0} + \frac{1}{\varsigma}\right)}{\sigma_n N_t v_{th}^n \left(1 + \frac{p_0}{n_0}\right)} \approx \frac{(1+\varsigma) + \left(\frac{v_{th}^n}{v_{th}^p}\right)\left(\frac{n_0}{p_0}\right)\left(1 + \frac{1}{\varsigma}\right)}{\sigma_n N_t v_{th}^n \left(1 + \frac{n_0}{p_0}\right)}$$

Results: Comparison of Theory with Experiment

n-HgCdTe

Assuming that all of the above recombination mechanisms operate independently, the total lifetime τ is determined from

$$\frac{1}{\tau} = \frac{1}{\tau_{Auger}} + \frac{1}{\tau_{Rad}} + \frac{1}{\tau_{SRH}}$$

For the calculation of these lifetimes, the carrier densities and Fermi level must be evaluated. At low temperature in doped material, the dopant energy level plays an important role in determining these quantities. We find that a donor level (E_D) at 7 meV above the conduction band edge provides an excellent fit to the measured carrier densities in all three *n*-type samples studied here, as shown in Figure 1(a). The first sample has x=0.224 with In doping of 4-5x10^{14} cm^{-3}, the second sample has x=0.232 and is nominally undoped with *n*= 2-3 x 10^{13} cm^{-3}, and the third sample has *x*=0.310 with In doping of 5x10^{14} cm^{-3}. Note that the variable field Hall

measurements were necessary to separate surface and interfacial conduction to give the appropriate carrier concentrations.[1]

Auger and radiative lifetimes for all three samples were calculated as described above, with this value of E_D, and compared with measured values. The calculated Auger lifetimes in all samples are found to be important only at higher temperatures, where the material is intrinsic, approximately 100 K for the narrow gap x=0.22 alloys and at about 200 K for the x=0.31 alloy. Our calculated Auger lifetimes at these higher temperatures agree within a factor of 2-3 with those predicted using the expression reported in Lopes et al.,[7] with an overlap integral of 0.2. However, at low temperatures, our calculated Auger calculations are an order of magnitude longer than does this expression, and consequently are insufficient to explain the measured lifetimes. In the narrow gap materials (x=0.224 and x=0.232) we find that the radiative lifetime does not contribute substantially to the recombination rate, even up to room temperature. However, in the wider gap $Hg_{0.69}Cd_{0.31}Te$, radiative recombination contributes throughout the temperature range examined. The radiative rates that we predict for this material differ from those calculated using the expression from Lopes et al. by a factor of ~2-3. A careful investigation revealed that accurate evaluation of the dipole matrix element accounts for only about 20% of the difference in the calculated radiative recombination rates, and the rest of the difference arises from detailed band structure effects. Because of the longer lifetimes predicted due to radiative and Auger recombination mechanisms compared with those predicted by the "standard" expressions, we conclude that significant SRH recombination must be present to explain the experimental data.

We calculated the SRH lifetime as a function of two unknowns, E_t and the product $N_t\sigma_p$, and combined this value with the radiative and Auger lifetimes to obtain total temperature-dependent

lifetimes. We assumed that the trap properties and density were comparable in all three samples. The values of E_t and $N_t\sigma_p$ were varied until we obtained a good fit to all of the data on the material subjected to a single step anneal. The calculated SRH and the total lifetimes are shown in Figure 1(b)-(d). The nearly perfect fit was possible with a value of $N_t\sigma_p = 0.8$ cm^{-1} in all three samples. However, the trap level (with reference to the conduction band edge) needed to be varied slightly with temperature to yield a good fit to the experimental lifetimes. All three samples can be fit with a trap state very close to the conduction band edge and tracking the temperature dependence of the conduction band minimum, as shown in Figure 2(a)-(c) for these three samples. For temperatures above 100 K, a smaller SRH rate is needed to fit the data. In the absence of any information about the nature of the traps, we chose an approach that allows the trap state to cross into the conduction band as the temperature is raised. Alternatively, this fit could be achieved by fixing the trap at the conduction band edge at $T>100$ K and allowing the $N_t\sigma_p$ to vary as a function of temperature at these higher temperatures.

The observed temperature dependence of the SRH lifetimes can be largely attributed to the temperature-dependence of the Fermi energy, also shown in Figure 2(a)-(c). In Figure 2(a)-(c), we have also plotted η. At low temperature, the first term in the numerator of expression for τ_{SRH} dominates. As the Fermi energy moves away from the trap state, η increases and consequently SRH lifetime increases. The maximum in the experimental lifetime data corresponds to the maximum in the $(1+\eta)$ factor. Although the lifetimes are not directly proportional to this factor, its exponential temperature dependence dominates the weaker temperature dependence from the denominator and from the second term, which begins to contribute only at the higher temperatures.

From Figure 2(d) it can be seen that the relative position of the Fermi energy with respect to the trap level (or conduction band edge) explains the observed temperature-dependence of the lifetimes in all three samples. In the x=0.224 sample, the Fermi energy moves away from the conduction band edge until T~100 K and then starts to move toward the conduction band edge. The observed lifetime increases until T~100 K and then starts to decrease. In both the x=0.232, $N_D=3x10^{13}$ cm^{-3} and the x=0.31 sample, the Fermi energy is closer to mid-gap (further from the trap level), and the SRH lifetime is consequently longer.

We see from Figure 2(d) that the dependence of the Fermi energy on temperature and x explains the observed lifetime variations, assuming a single trap whose level is close to and tracks the conduction band edge. A number of candidate defects could be giving rise to this state. One possibility is that it is an extrinsic impurity that is introduced from the source material or during the growth or post-growth processing of the materials. Another possibility is that it is an intrinsic defect. The tellurium antisite is a candidate, since it has been predicted to have a donor-like state in the band gap and to be present in densities of ~10^{12} cm^{-3} in MBE-grown material.[17] Although the density of the antisites should be reduced far below this density if it is fully equilibrated under the Hg-saturated annealing conditions, it is plausible that the time needed to equilibrate this defect is much longer than the 10 hours at 245°C used in the one-step anneal in these experiments.

Another candidate for the trap is the ionized donors themselves. Since this could be potentially most damaging for electronic and sensor applications (since it will always be present in doped materials), we investigated this possibility further. The SRH calculations were repeated with the donor energy level coinciding with the trap energy level. The lifetimes calculated in x=0.224 alloy with $E_D=E_T=0$ meV and $E_D=E_T=7$ meV (into the conduction band) are compared with

experiments in Figure 3(a). We see that a 7 meV trap/donor level, while predicting electron concentrations in good agreement with experiment (shown in Figure 3(b)), predicts lifetimes that are in poor agreement with the measured values. On the other hand, calculations using a trap/donor level at the conduction band minimum predict lifetimes comparable to the experimental values, but predict carrier freeze out at low temperatures, as shown in Figure 3(b). Since carrier freeze-out has not been observed in any of *n*-type HgCdTe sample, we rule out the possibility of the donor-traps scenario.

The identification of the SRH defect with a native defect is suggested by the lifetime data on the low x material subjected to the two-step anneal, which displays longer minority carrier lifetimes, as shown in Figure 4. Because the SRH recombination is the primary lifetime-limiting mechanism at $T > 100$ K, the increase in lifetimes in the materials subjected to a two step anneal can be correlated with a decrease in the number of SRH centers.[18]

p-type

Similar calculations were carried out and compared with measured minority carrier (electron) lifetimes in nominally 2 x 10^{16} cm^{-3} *p*-doped $Hg_{0.7}Cd_{0.3}Te$ alloy. The use of an acceptor level of 11 meV above the valence band edge yielded an excellent agreement with the measured carrier density, as seen in Figure 5(a). Owing to high mobility of electrons, multiple carrier analysis of Hall data is needed to obtain accurate hole density. Since the doping density is relatively high, the material does not become intrinsic even at 250 K, and the calculated carrier density is nearly constant for a large temperature range. Notice that the calculations agree with measured values for both holes and thermal generation of intrinsic electrons (as measured by quantitative mobility spectrum analysis). Although the hole density is nearly constant at high temperatures, the Auger lifetime shows variation because of a change in the band gap, as shown in Figure 5(b)

Consequently, the Auger mechanism becomes more effective only at very high temperatures. In this medium gap alloy, the radiative lifetime is important, but is not found to be the lifetime-limiting mechanism. As before, SRH scattering is required to obtain a good agreement between the calculated and measured lifetimes. SRH is the limiting mechanism at low temperatures. At higher T, both the radiative and Auger mechanisms become important, and we could get an excellent fit to the experiments. With $N_t\sigma_n$=0.1 cm^{-1} and a trap level of E_T=76 meV (above the valence band edge) the calculated lifetimes nearly perfect fit to the measured lifetimes, as seen in Figure 5(b). The calculated Fermi energy and the function $\varsigma = e^{-\beta(E_t - F_0)}$ along with the fit trap energy level are shown in Figure 5(c). At low temperatures, where the Fermi energy is close to the trap level, ζ is small. We see from Figure 5(d) that with an increase in temperature, the Fermi energy moves away from the valence band edge. As seen in Fig. 5(d), as the temperature increases, ζ increases, resulting in longer SRH lifetimes. The SRH mechanism contributes substantially to the lifetime over the complete temperature range studied here.

Conclusions

The full band calculations indicate that the radiative and Auger recombination rates are much slower than those predicted by expressions used in the literature, and that SRH centers must be present in the MBE samples considered here. We have used a generalized expression for the SRH recombination lifetimes in degenerately doped material, and evaluated the radiative and Auger lifetimes using an accurate band structure. When the SRH center is assumed to be the same in all three samples subjected to an *n*-type anneal, we find a unique fit to the lifetime data with $N_t\sigma_p \approx 0.8$ cm^{-1} and a trap level that roughly tracks the temperature dependence of the conduction band edge. For p-type material, $N_t\sigma_n \approx 1.0$ cm^{-1} and a trap level at 75 meV above

valence band edge explains the measured lifetimes. However, in fitting the data, we did find that alternative choices of $N_t\sigma_t$ and $E_t(T)$ fit the data, for a particular concentration or for a limited temperature range. If we constrain the fit to data in the entire temperature range for all three *n*-type materials and assume that there is a similar density of the same SRH center in each sample, we find a unique fit with $N_t\sigma_p$ and $E_t(T)$ only in the range that we have reported here. Although the exact position of the trap level cannot be deduced from this work, due for example to the assumption that $\sigma_n \approx \sigma_p$, we can conclude that the data can be explained only with a trap level near to and roughly tracking the temperature dependence of the conduction band edge in *n*-doped alloys and tracking the valence band edge in the *p*-doped MCT alloys. It is also possible that both SRH levels that we fit are present in both the *n*- and *p*-type samples and that only those near the Fermi level affect the lifetimes. We find that the temperature-dependent Fermi energy with reference to the trap level explains the observed lifetime variations across samples with different band gaps, doping concentrations, and majority carrier types.

We have shown that the relative position of the trap level with respect to the Fermi energy is the important factor in determining the strength of a SRH center, and that consequently the near band edge trap states (rather than the mid-gap states) are important. This conclusion is *not* in contradiction with Shockley's original conclusion.[16] At high temperatures or in wider gap materials, where Shockley and Read applied that formalism, the Fermi energy is near the mid-gap, and thus the trap states near mid gap – and thus the Fermi energy -- are more important.

Acknowledgments

This work was supported by the Electro-Optics Center and Air Force Materials Laboratory at Wright-Patterson AFB. (Contract No. N00014-99-2-0005)

References

1. C. H. Swartz, R. P. Tompkins, N. C. Giles, T. H. Myers, D. D. Edwall, J. Ellsworth, E. Piquette, J. Arias, M. Berding, S. Krishnamurthy, I. Vurgaftman, and J. R. Meyer, Accepted for publication in *J. Electron. Mater.*
2. S. Krishnamurthy and M.A. Berding, *J. Appl. Phys*. **90** 828 (2001).
3. A.-B. Chen and A. Sher, *Semiconductor Alloys* (New York; Plenum, 1995).
4. G. L. Hansen, J. L. Schmit, and T. N. Casselman, *J. Appl. Phys.* **53**, 7099 (1982).
5. G. L. Hansen and J. L. Schmit, *J. Appl. Phys.* **54**, 1639 (1983).
6. W. van Roosbroeck and W. Shockley, *Phys. Rev.* **94,** 1558 (1954).
7. V. C. Lopes, A. J Syllaios, and M C. Chen, *Semicond. Sci. Technol***. 8**, 824 (1993).
8. S. E. Schacham and E. Finkman, *J. Appl. Phys.* **57**, 2001 (1985).
9. In narrow-gap HgCdTe, the conduction band is not effective mass-like except just at the band edge. Furthermore, as discussed in Schacham and Finkman, the absorption coefficient used in deriving the radiative recombination rate expression reported in Lopes does not agree with measured absorption data on narrow-gap HgCdTe, nor is the temperature dependence correct.
10. S. Krishnamurthy, A.-B. Chen, and A. Sher, *J. Appl. Phys.* **80**, 4045 (1996).
11. J. S. Blakemore, *Semiconductor Statistics* (New York; Dover Publications, Inc. 1986).
12. P. E. Petersen, *J. Appl. Phys***. 41,** 3465 (1970).
13. S. Krishnamurthy, A. Sher, and A.-B. Chen, *J. Appl. Phys*. **82**, 5540 (1997).
14. S. Krishnamurthy, A.-B. Chen, and A. Sher, *J. Electron. Mater.* **27**, 694 (1998); S. Krishnamurthy and T. N. Casselman, *J. Electron. Mater.* **29**, 828 (2000).
15. S. M. Sze, *Physics of Semiconductor Devices* (New York; John Wiley & Sons, 1981).
16. W. Shockley and W. T. Read, *Phys. Rev*. **87**, 835 (1952); R. N. Hall, *Phys. Rev*. **87**, 387 (1952).
17. M. A. Berding, M. van Schilfgaarde, and A. Sher, *Phys. Rev. B* **50,** 1519 (1994).
18. Note that the carrier concentrations are found to be lower in the two-step annealed samples. The SRH lifetimes would have to be refit with this new carrier concentration to deduce the magnitude of the reduction of the trap density.

Figure Captions:

Figure 1. (a) Comparison of experimental carrier density (symbols) and the calculated carrier density of various *n*-type samples, assuming a donor energy level that is 7 meV into the conduction band. (b)-(d) The calculated Auger, radiative, SRH, and total lifetimes compared to experimental lifetimes (symbols) for the same samples.

Figure 2. Calculated Fermi energy and fitted trap energy with respect to the conduction band edge, and η–factor, for (a) x=0.224, 4-5x10^{14} cm^{-3} *n*-doped, (b) x=0.232, 2-3x10^{13} cm^{-3} *n*-type, and (c) x=0.310, 5x10^{14} cm^{-3} *n*-doped HgCdTe alloys. (d) The measured lifetime and calculated Fermi energy and variations in the same three alloys.

Figure 3. (a) Lifetimes and (b) electron density calculated with E_D=E_T=0 meV and E_D=E_T=+7 meV (i.e., into the conduction band) with respect to the conduction band edge, compared with experimental values.

Figure 4. Lifetime in three samples with one-step anneal (thick line) and two-step anneal (thin line) discussed in text. *x*=0.31 material subjected to one-step anneal only.

Figure 5: (a) Comparison of calculated and measured hole density in x=0.30, N_A= 2 x10^{16} cm^{-3} *p*-doped HgCdTe. (b) The calculated Auger, radiative, SRH, and total lifetimes compared to experimental lifetimes (symbols) for the same sample. (c). Calculated Fermi energy and fitted trap energy with respect to the valence band edge, and η–factor, for the same sample. (d) Calculated Fermi energy and fitted trap energy with respect to the valence band edge, and the measured lifetime variations in this alloy.

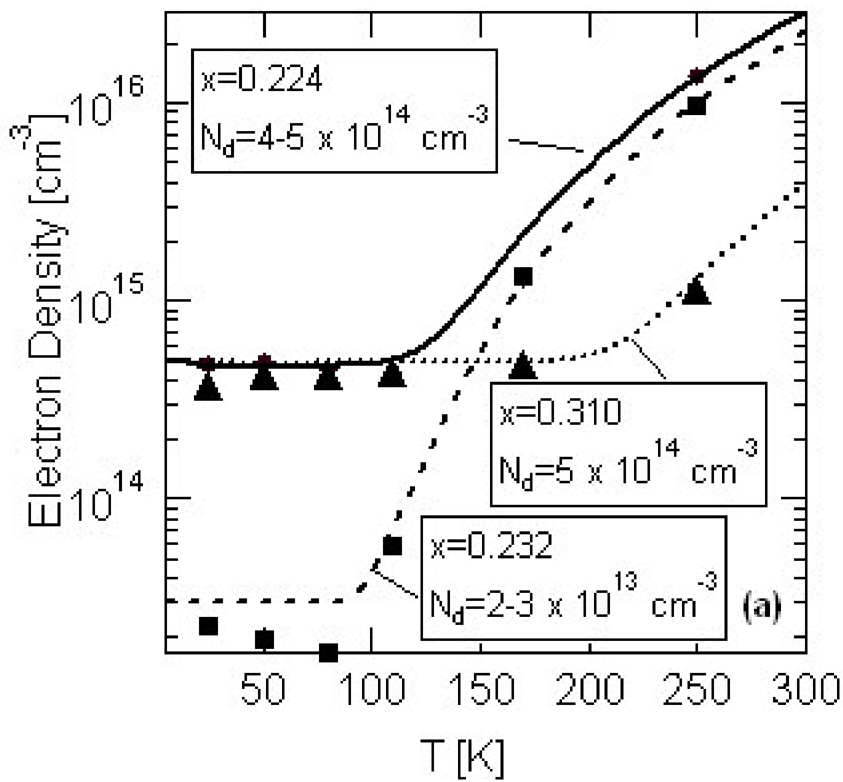

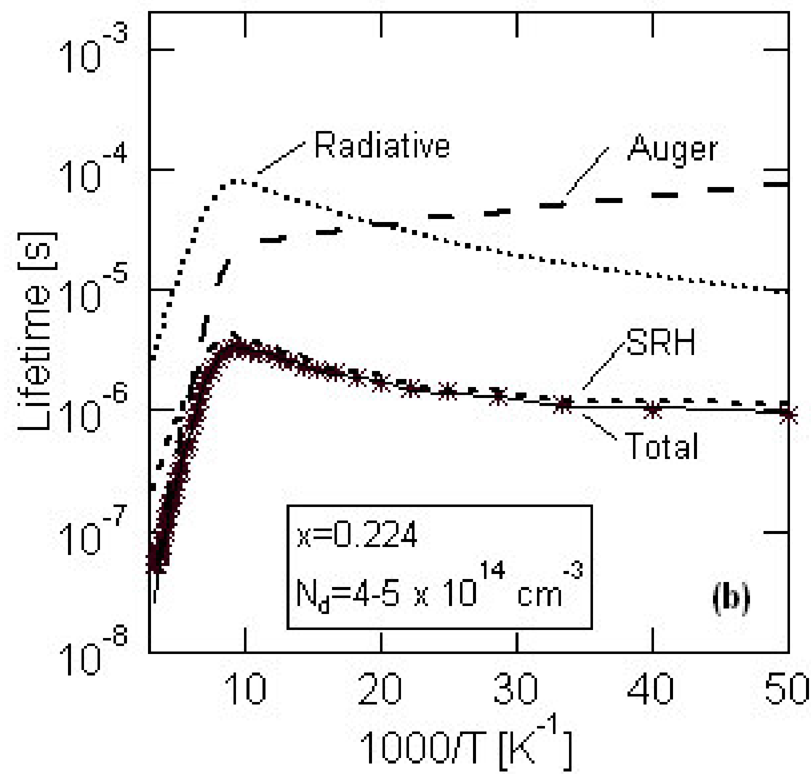

FIGURE 1

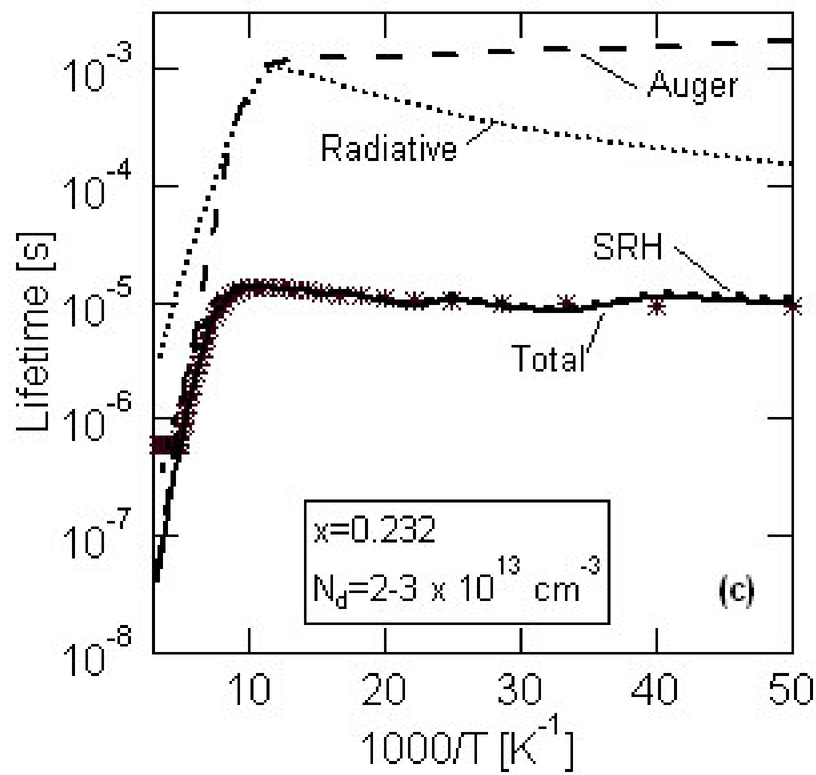

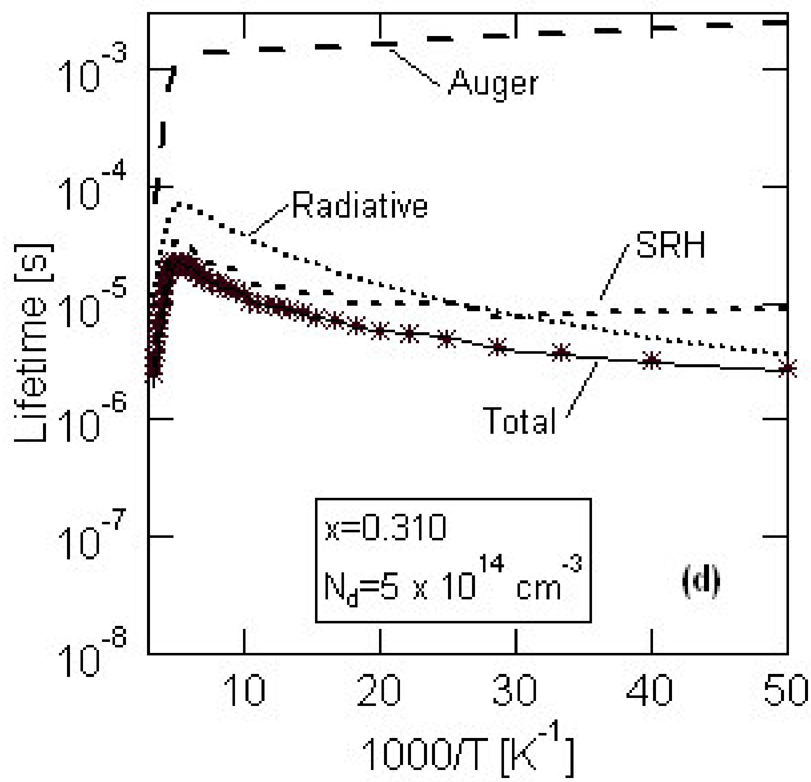

FIGURE 1

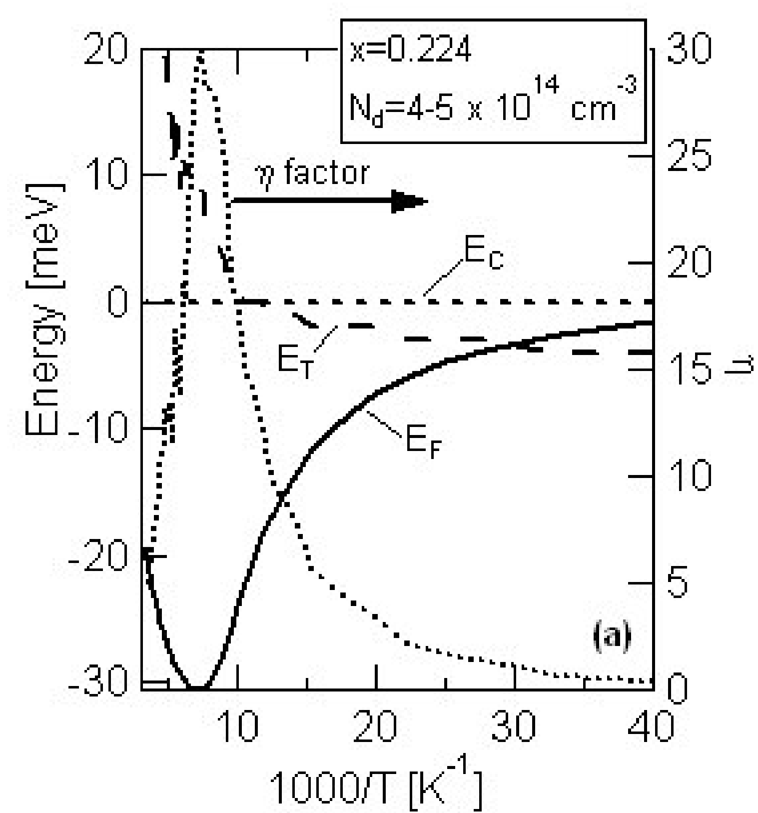

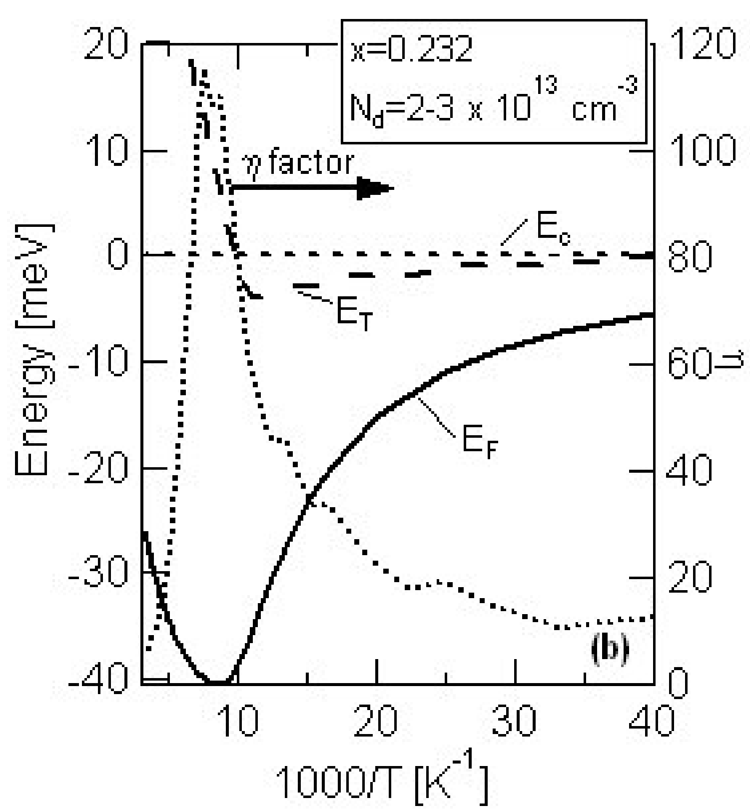

FIGURE 2

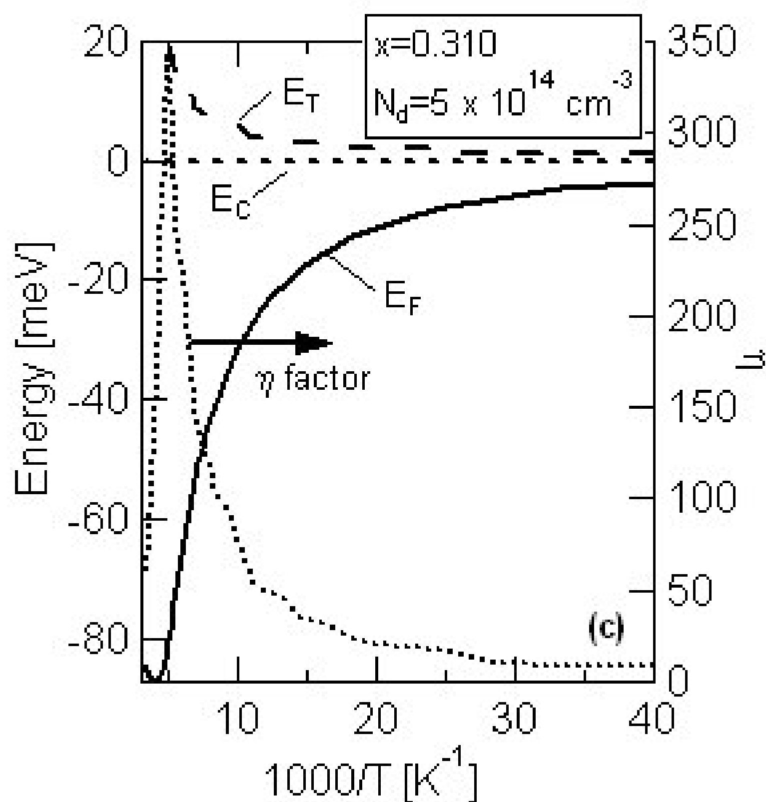

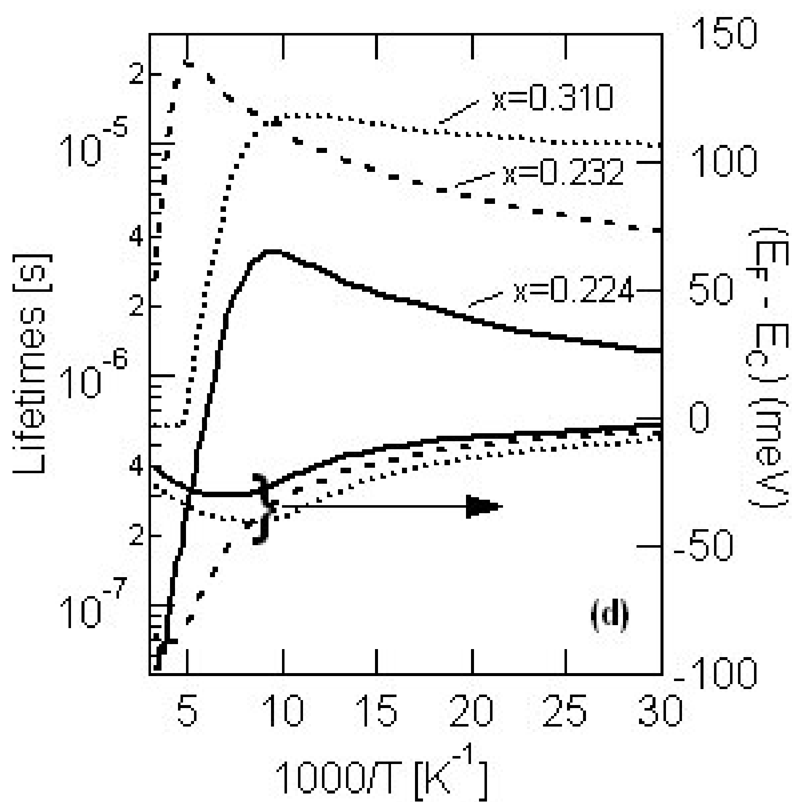

FIGURE 2

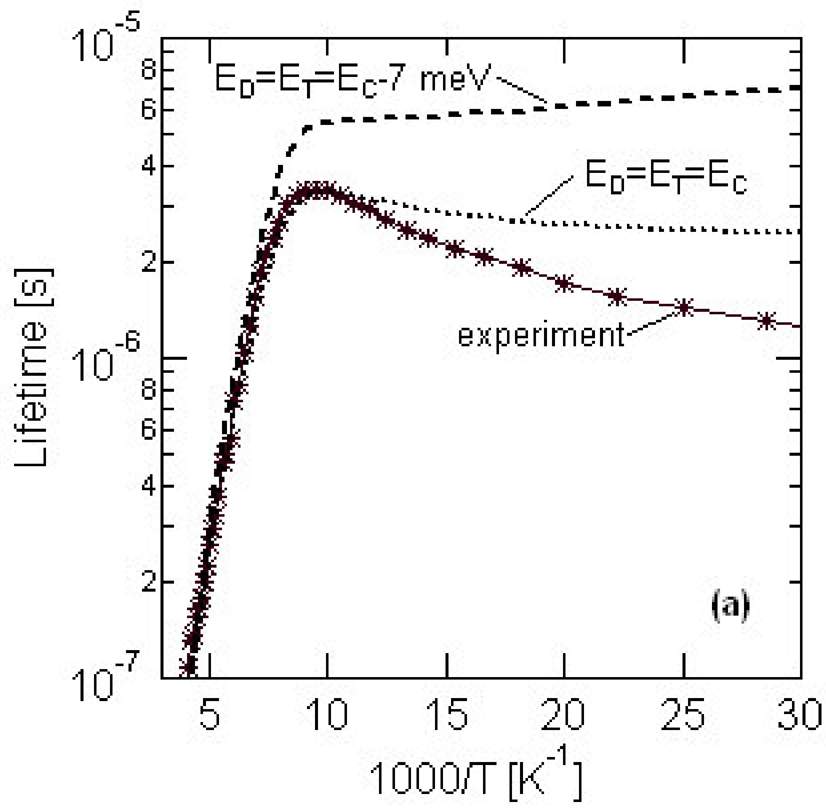

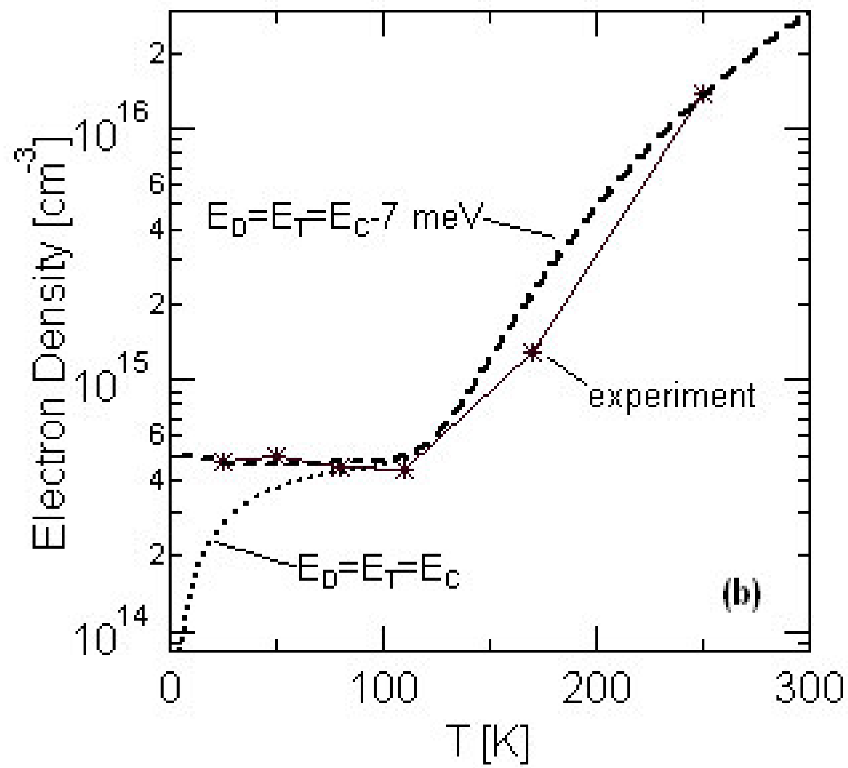

FIGURE 3

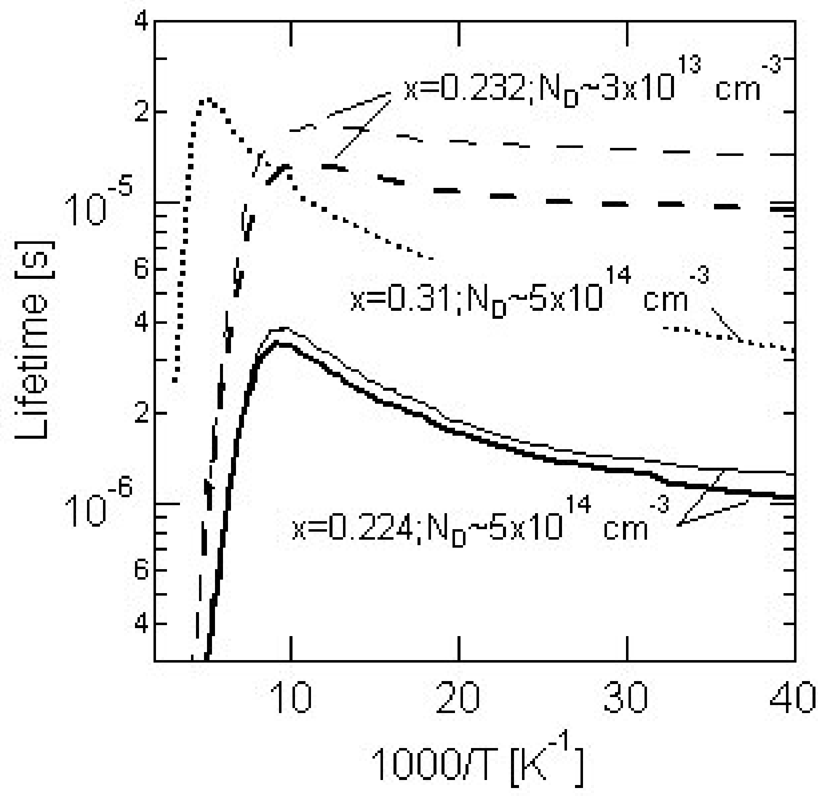

FIGURE 4

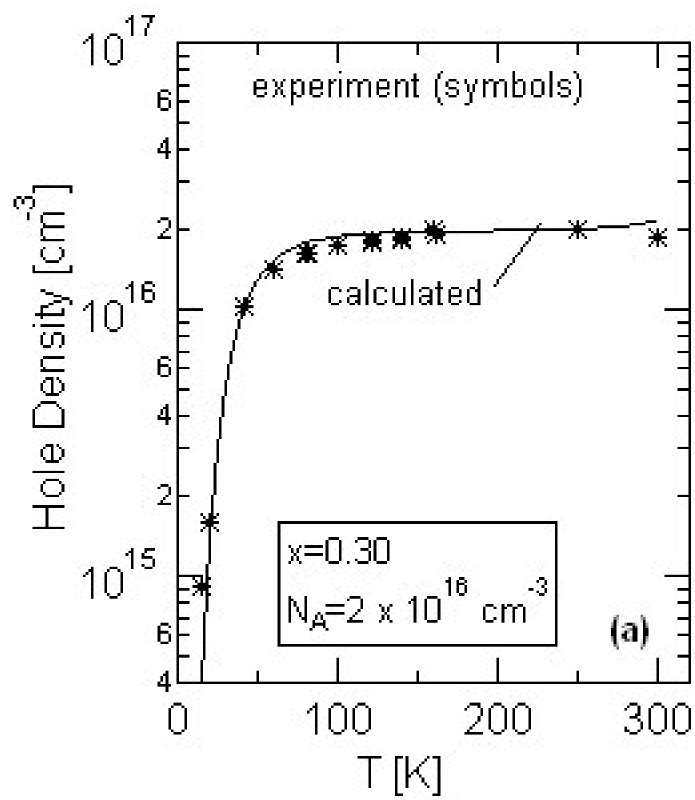

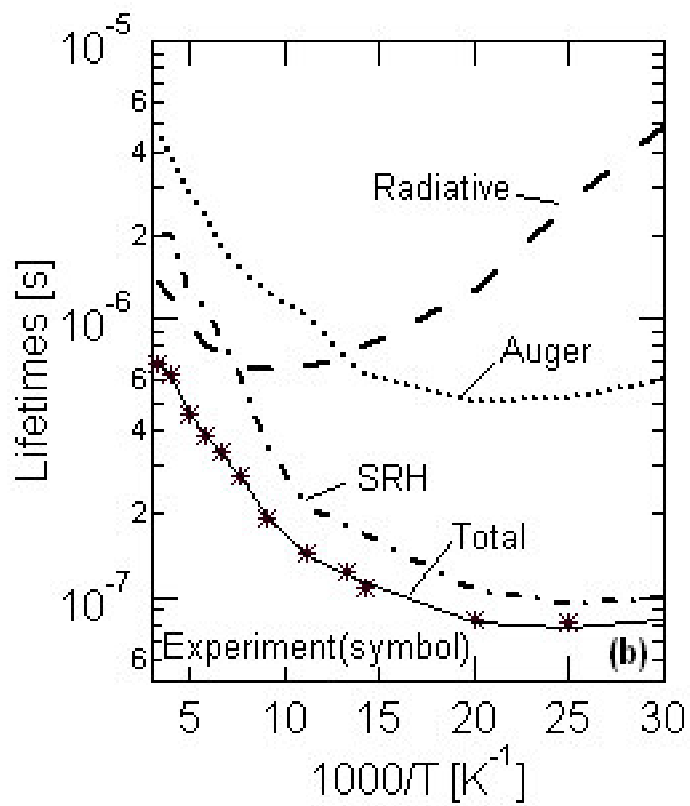

FIGURE 5

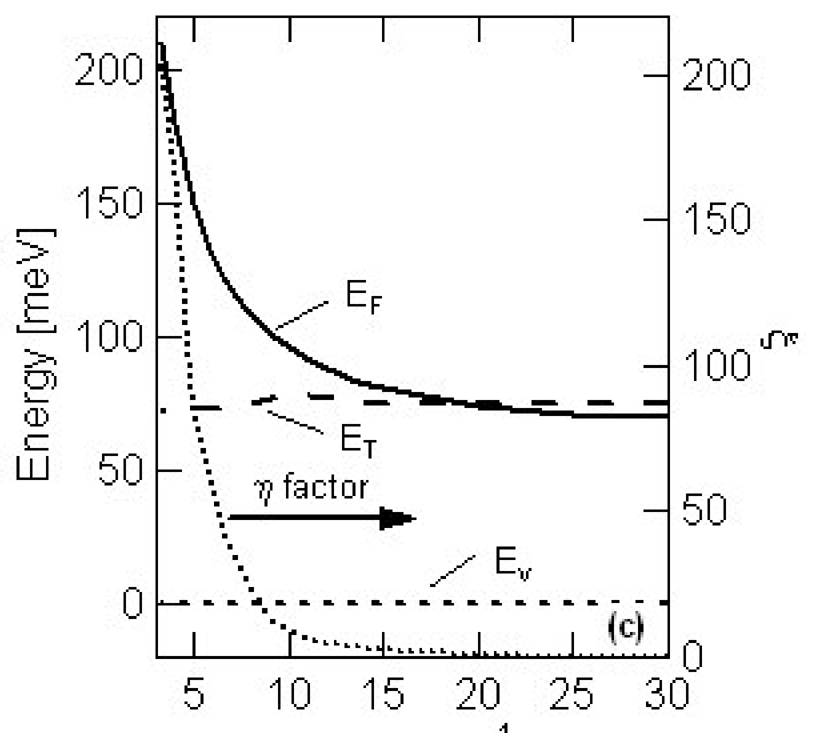

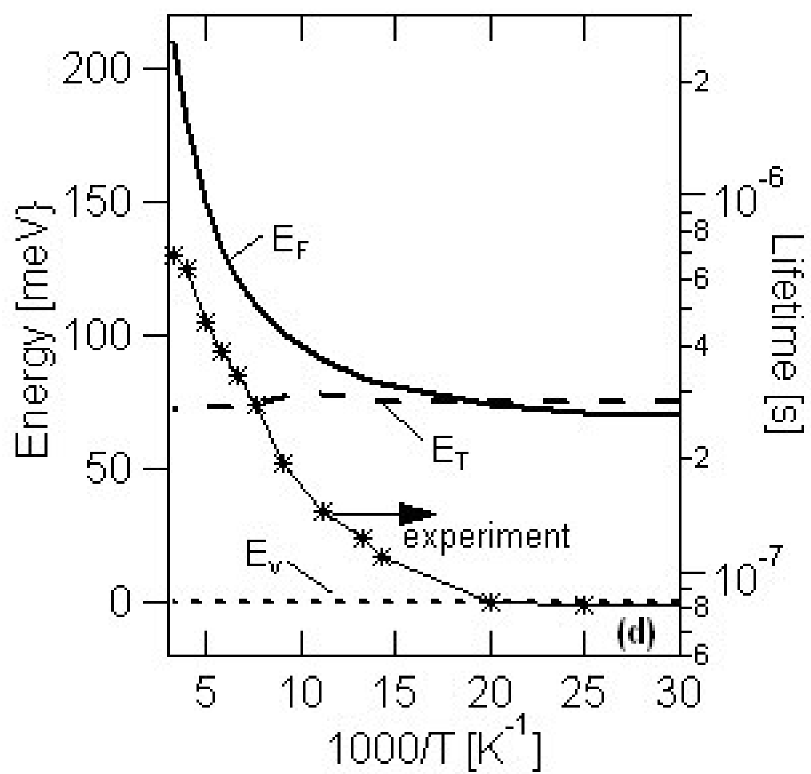

FIGURE 5